

# Transmitter Precoding for ICI Reduction in Closed-Loop MIMO OFDM Systems

Yu Fu, Chintha Tellambura, *Senior Member, IEEE*, and Witold A. Krzymień, *Senior Member, IEEE*

**Abstract**—The mitigation of intercarrier interference (ICI) in closed-loop single-input–single-output (SISO) and multiple-input–multiple-output (MIMO) orthogonal frequency-division multiplexing (OFDM) is considered. The authors show that the ICI coefficient matrix is approximately unitary and exploit this property to design a nonlinear Tomlinson–Harashima precoder for the reduction of ICI in closed-loop SISO OFDM and orthogonal space-time block-coded (OSTBC) MIMO OFDM. With the proposed design, the transmitter does not need to know the frequency offsets, and hence, their impact on the bit error rate (BER) is significantly reduced. Moreover, for spatially correlated MIMO channels, the precoder and OSTBC OFDM perform with a negligible BER-performance loss.

**Index Terms**—Closed loop, frequency offset, multiple-input–multiple-output (MIMO), orthogonal frequency-division multiplexing (OFDM), Tomlinson–Harashima (TH) precoder.

## I. INTRODUCTION

CURRENT trends in the development of high-data-rate wireless systems focus on the integration of orthogonal frequency-division multiplexing (OFDM), multiple-input–multiple-output (MIMO), and closed-loop techniques [1] and [2]. When perfect channel state information (CSI) is available at the transmitter, closed-loop single-input–single-output (SISO) and MIMO systems perform significantly better than their open-loop counterparts and, hence, have been proposed in the third generation 3G cellular standards, including wide-band code-division multiple access (W-CDMA) and cdma2000 [3], [4]. In closed-loop systems, transmit precoding reacts to channel conditions in order to improve the system capacity or bit error rate (BER). For instance, closed-loop MIMO OFDM allows transmit precoding on frequency-selective channels to preprocess signals at the subcarrier level and facilitates the utilization of capacity or performance gain. When free of channel distortions, orthogonal OFDM subcarriers are fully separable by a discrete Fourier transform (DFT) at the receiver. However, a carrier frequency offset may exist because of mismatch of oscillators and/or the Doppler shift caused by the relative

motion between the transmitter and receiver or movement of other objects around transceivers. Such frequency offsets distort the orthogonality between subcarriers and result in intercarrier interference (ICI) [5]. To the best of our knowledge, the issue of how ICI impacts the performance of closed-loop OFDM systems has not been studied yet.

The availability of CSI at the transmitter is a primary requirement for closed-loop systems. Complete CSI in this case includes both the frequency offsets and channel response. In closed-loop MIMO OFDM, if complete CSI is available at the transmitter, precoding can be designed to exploit the channel conditions, avoid interference, and reduce the complexity at the receiver. For instance, when the time-division duplex (TDD) mode is used, the channel response can be estimated at the transmitter by exploiting the approximate reciprocity between the forward and reverse channels. Alternatively, the channel response estimated at the receiver can be sent back to the transmitter via a feedback link [6]. Nevertheless, all the distinct frequency offsets among multiple antennas may not be readily obtained at the transmit end. In a TDD system, the frequency offsets may not be directly estimated at the transmitter. In frequency-division duplex (FDD) systems, where the forward and reverse links are not reciprocal, the feedback capacity is usually limited. Imperfect channel and frequency-offset feedback, which causes residual ICI, increases the BER.

In this paper, we propose a nonlinear Tomlinson–Harashima (TH) precoder for mitigating ICI in closed-loop SISO and orthogonal space-time block-coded (OSTBC) OFDM systems when only partial CSI (no knowledge of frequency offsets) is available at the transmitter. TH precoding (THP) is a transmitter-based preequalization technique, which was originally proposed for temporal equalization in conventional SISO systems [7], [8], and has recently been extended to flat-fading MIMO channels in [9]–[11] to combat the interlayer interference. The TH precoder enables the receiver to reliably estimate the data symbols without the noise enhancement typical of the zero-forcing (ZF) precoder or minimum mean-square-error (MMSE) linear precoder, and without the error propagation typical of the decision feedback equalizer (DFE). We first show that except for the most general case, where all the frequency offsets are distinct, the ICI coefficient matrix is approximately unitary. Consequently, the proposed transmit precoder does not need to know the frequency offset. This avoids feedback in a TDD system, where the estimation of frequency offsets may be difficult at the transmitter. In FDD systems, this unitary property leads to savings of feedback capacity since a MIMO system may experience a set of distinct frequency offsets. Frequency-offset mismatch due to imperfect feedback is also avoided.

Manuscript received November 24, 2005; revised February 16, 2006. This work was supported by Natural Sciences and Engineering Research Council (NSERC) of Canada and TRILabs. This work was presented in part at the 61st IEEE Vehicular Technology Conference (VTC'05-Spring), Stockholm, Sweden, May 2005. The review of this paper was coordinated by Prof. X.-G. Xia.

Y. Fu and C. Tellambura are with the Department of Electrical and Computer Engineering, University of Alberta, Edmonton, AB T6G 2V4, Canada (e-mail: yufu@ece.ualberta.ca; chintha@ece.ualberta.ca).

W. A. Krzymień is with the Department of Electrical and Computer Engineering, University of Alberta, Edmonton, AB T6G 2V4, Canada, and also with the TRILabs, Edmonton, AB T6G 2V4, Canada (e-mail: wak@ece.ualberta.ca).

Digital Object Identifier 10.1109/TVT.2006.883782

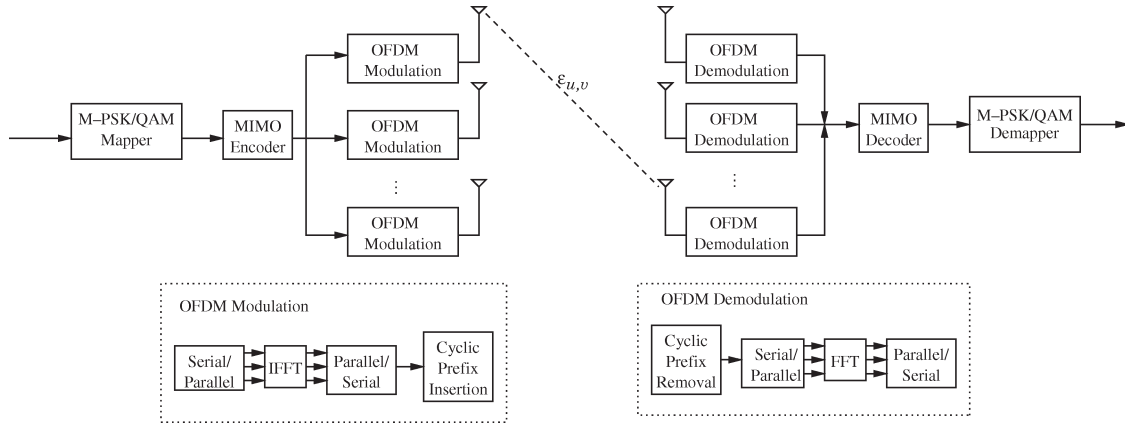


Fig. 1. Block diagram of a MIMO OFDM link.

Consequently, our precoder significantly suppresses the BER increase due to frequency offsets. Since practical MIMO channels may experience spatially correlated fading, we study how the proposed THP and an OSTBC MIMO OFDM system perform over such channels; we find that the combined system is robust against spatial correlation, and the BER increase is negligible.

Previous work on ICI reduction has focused on open-loop OFDM (the CSI is not available at the transmitter but only at the receiver). For open-loop SISO OFDM, ICI can be reduced using an optimum time-domain Nyquist windowing function, selective mapping and partial transmit sequences, and MMSE filtering employing finite power series expansion of the time-varying frequency response [12]–[14]. Other methods include a two-stage ICI-suppressing equalizer [15], which applies linear preprocessing at the transmitter and an iterative MMSE estimator at the receiver, and self-cancellation schemes [16], [17] involving mapping of each input symbol to a group of subcarriers at a price of reducing the bandwidth efficiency. For open-loop MIMO OFDM, a bank of time-domain ICI cancellation filters has also been proposed to maximize the per-symbol ratio of signal energy to ICI-plus-noise energy [18].

### A. Organization of the Paper

This paper is organized as follows. In Section II, we describe a MIMO OFDM system model in the presence of frequency offsets. Section III discusses the ICI coefficient-matrix properties that are exploited to design a new nonlinear TH precoder for both SISO and OSTBC OFDM. The effect of channel mismatch on THP is also studied. A spatially correlated MIMO channel model is introduced in Section IV. Simulation results of SISO and MIMO OFDM are given in Section V. Section VI concludes the paper.

### B. Notation

The superscripts  $\text{T}$ ,  $\text{H}$ ,  $*$ , and  $\dagger$  stand for transposition, conjugate transposition, element-wise conjugate, and Moore–Penrose pseudo inverse, respectively. Bold symbols denote matrices or vectors. The symbol  $\otimes$  represents the Kronecker product, and  $\delta(\cdot)$  represents Kronecker delta. The expectation operator is  $E$ .  $j = \sqrt{-1}$ . The  $N \times N$  identity matrix is  $\mathbf{I}_N$ .

The  $M \times N$  all-zero matrix is  $\mathbf{0}_{M \times N}$ . The  $m$ th row and  $n$ th column entry of  $\mathbf{A}$  are denoted as  $A(m, n)$ . The trace of  $\mathbf{A}$  is given as  $\text{tr}(\mathbf{A}) = \sum_m A(m, m)$ . The  $\Re(a)$  and  $\Im(a)$  indicate the real and imaginary part of a complex number  $a$ . An  $M$ -ary quadrature amplitude modulation (QAM) square signal constellation is defined as  $\mathcal{A} = \{a_I + ja_Q | a_I, a_Q \in \pm 1, \pm 3, \dots, \pm(\sqrt{M} - 1)\}$ .

## II. SYSTEM MODEL

This section will introduce the MIMO OFDM system model in the presence of frequency offsets. This model can also be simplified to SISO OFDM systems.

We consider an OFDM system with  $M_T$  transmit antennas and  $M_R$  receive antennas (Fig. 1). Let  $X_u[n]$  denote an  $M$ -ary QAM symbol on the  $n$ th subcarrier sent by the  $u$ th transmit antenna. The length- $N$  input data vector can then be written as  $\mathbf{X}_u = [X_u[0]X_u[1] \cdots X_u[N-1]]^T$ , where  $N$  is the number of OFDM subcarriers. In MIMO OFDM transmission, each of the  $M_T$  time-domain transmitted vectors is generated by taking an inverse DFT (IDFT) of an information vector:

$$\mathbf{x}_u = [x_u(0)x_u(1) \cdots x_u(N-1)]^T = \mathbf{Q}\mathbf{X}_u \quad (1)$$

where  $\mathbf{Q}$  is the  $N \times N$  IDFT matrix with entries  $Q(m, n) = (1/N) \exp[j(2\pi/N)mn]$ . A cyclic prefix, which is longer than the expected maximum excess delay, is customarily inserted at the beginning of each time-domain OFDM symbol to prevent intersymbol interference.

Considering a wideband frequency-selective fading channel with  $L$  resolvable paths between the  $u$ th transmit antenna and  $v$ th receive antenna, the discrete-time-domain received signal can be represented as

$$y_{u,v}(k) = e^{j\frac{2\pi}{N}\varepsilon_{u,v}k} \sum_{l=0}^{L-1} h_{u,v}(l)x_u(k-l) + w_{u,v}(k) \quad (2)$$

where  $\varepsilon_{u,v} = \Delta f_{u,v}T_s$  is the normalized frequency offset between the  $u$ th ( $u = 1, \dots, M_T$ ) transmit and  $v$ th ( $v = 1, \dots, M_R$ ) receive antenna; the  $\Delta f_{u,v}$  is the frequency offset, and  $T_s$  is the OFDM symbol period. The  $w_{u,v}(k)$  is an additive white Gaussian noise (AWGN) sample. The complex channel gain  $h_{u,v}(l)$ ,  $l = 0, 1, \dots, L-1$  refers to the  $l$ th path between

the  $u$ th transmit and  $v$ th receive antenna. Each path gain is a zero-mean complex Gaussian random variable (Rayleigh fading) with variance  $\sigma_l^2$  (see Section V for details). We assume that the channel gains remain constant over several OFDM symbol intervals.

Discarding the cyclic prefix and performing DFT on the received samples, the signal received at the  $v$ th receive antenna for the  $k$ th subcarrier is given by

$$Y_v[k] = \underbrace{\sum_{u=1}^{M_T} S_{u,v}[0]H_{u,v}[k]X_u[k]}_{\text{desired signal}} + \underbrace{\sum_{u=1}^{M_T} \sum_{n=0, n \neq k}^{N-1} S_{u,v}[n-k]H_{u,v}[n]X_u[n]}_{\text{ICI component}} + \sum_{u=1}^{M_T} W_{u,v}[k] \quad (3)$$

for  $k = 0, 1, \dots, N-1$ , where  $W_{u,v}[k]$  is an AWGN sample with zero mean and variance  $\sigma_W^2$ , and  $W_{u,v}[k], \forall k$  are assumed independent and identically distributed (i.i.d);  $H_{u,v}[k] = \sum_{l=0}^{N-1} h_{u,v}(l)e^{-j(2\pi/N)lk}$ , and  $S_{u,v}[n-k]$  is an ICI coefficient given by

$$S_{u,v}[m] = \frac{\sin \pi(\varepsilon_{u,v} + m)}{N \sin \frac{\pi}{N}(\varepsilon_{u,v} + m)} e^{j\pi(1-\frac{1}{N})(\varepsilon_{u,v} + m)} \quad (4)$$

for  $m = 1-N, \dots, 0, \dots, N-1$ ,  $u = 1, \dots, M_T$ , and  $v = 1, \dots, M_R$ . All received signals can therefore be represented in matrix form as

$$\mathbf{Y} = \mathbf{S}\mathbf{H}\mathbf{X} + \mathbf{W} = \mathbf{G}\mathbf{X} + \mathbf{W} \quad (5)$$

where the  $NM_R$ -dimensional vector  $\mathbf{Y} = [Y_1[0] \cdots Y_1[N-1] \cdots Y_{M_R}[N-1]]^T$ ; the  $NM_T \times 1$  transmitted vector  $\mathbf{X} = [\mathbf{X}_1^T \cdots \mathbf{X}_{M_T}^T]^T$ ; the noise vector  $\mathbf{W}$  with the  $\{(v-1)N+k\}$ th entry  $W_v[k] = \sum_{u=1}^{M_T} W_{u,v}[k], \forall k, v$ . The  $NM_R \times NM_T$  overall channel matrix is  $\mathbf{G} = \mathbf{S}\mathbf{H}$ , where  $\mathbf{S}$  is an  $NM_R \times NM_R M_T$  ICI matrix

$$\mathbf{S} = \text{diag}[\mathbf{S}_1 \cdots \mathbf{S}_{M_R}] \quad (6)$$

with  $\mathbf{S}_v = [\mathbf{S}_{1,v} \cdots \mathbf{S}_{M_T,v}]$ ; the  $\{u, v\}$ th element is the ICI coefficient matrix between the  $u$ th transmit and  $v$ th receive antenna

$$\mathbf{S}_{u,v} = \begin{bmatrix} S_{u,v}[0] & S_{u,v}[1] & \cdots & S_{u,v}[N-1] \\ S_{u,v}[-1] & S_{u,v}[0] & \cdots & S_{u,v}[N-2] \\ \vdots & & \ddots & \vdots \\ S_{u,v}[1-N] & S_{u,v}[2-N] & \cdots & S_{u,v}[0] \end{bmatrix} \quad (7)$$

and  $\mathbf{H}$  is an  $NM_R M_T \times NM_T$  channel-gain matrix, which is given by

$$\mathbf{H} = [\mathbf{H}_1 \cdots \mathbf{H}_{M_R}]^T = \begin{bmatrix} \mathbf{H}_{1,1} & \cdots & \mathbf{0} & \cdots & \mathbf{H}_{1,M_R} & \cdots & \mathbf{0} \\ \vdots & \ddots & \vdots & & \vdots & \ddots & \vdots \\ \mathbf{0} & \cdots & \mathbf{H}_{M_T,1} & \cdots & \mathbf{0} & \cdots & \mathbf{H}_{M_T,M_R} \end{bmatrix}^T \quad (8)$$

where  $\mathbf{H}_v = \text{diag}[\mathbf{H}_{1,v} \cdots \mathbf{H}_{M_T,v}]$  and where the elements are the  $\{u, v\}$ th channel-gain matrix  $\mathbf{H}_{u,v}$  at the  $N$  orthogonal subcarriers

$$\mathbf{H}_{u,v} = \text{diag}[H_{u,v}[0] \quad H_{u,v}[1] \quad \cdots \quad H_{u,v}[N-1]]. \quad (9)$$

When  $M_T = 1$  and  $M_R = 1$ , (5) reverts to the system model for SISO OFDM systems.

### III. PRECODING FOR ICI REDUCTION

Let us consider precoding for OFDM ICI reduction. For completeness, we briefly discuss linear precoding, which needs the complete CSI (including frequency-offset information) at the transmitter. As discussed in the Introduction, the provision of frequency-offset estimates at the transmit end is difficult. A nonlinear TH precoder to suppress ICI for both SISO and MIMO OFDM with only partial CSI at the transmitter is therefore proposed, where partial refers to the fact that the transmitter does not need to know the frequency offsets. We also analyze how channel mismatch impacts the TH precoder.

#### A. Linear Precoding

For linear transmitter precoding, an  $NM_T \times NM_R$  ( $M_T \geq M_R$ ) transformation matrix  $\mathbf{L}$  is used to preprocess transmitted symbols so that  $\mathbf{L}\mathbf{X}$  instead of  $\mathbf{X}$  is transmitted. The matrix  $\mathbf{L}$  depends on the overall channel conditions and several performance criteria. With the ZF criterion, we choose  $\mathbf{G}\mathbf{L}_{\text{ZF}} = \mathbf{I}$ , i.e.,  $\mathbf{L}_{\text{ZF}} = \mathbf{G}^\dagger$ ; ICI is thus completely eliminated. In practical implementation, the average transmit power for each OFDM symbol should be constant, and large fluctuations are undesirable, i.e.,  $(1/M_T)E[\mathbf{L}\mathbf{X}\mathbf{X}^H\mathbf{L}^H] = (E_s/M_T)\mathbf{L}\mathbf{L}^H$ , where  $E_s = E[|X[k]|^2], \forall k$ , should be constant. However, the channel inverse  $\mathbf{G}^\dagger$  not only increases the average transmit power but also makes it variable from symbol to symbol. Moreover, if the channel transfer function has zeros outside the unit circle, the system will be unstable. To alleviate these problems, one can design a linear precoder subject to a power constraint. Under the power constraint  $E_L$  and with the MMSE criterion, we have  $\mathbf{L}_{\text{MMSE}} = \sqrt{E_L/NM_T}\mathbf{G}^H (\mathbf{G}\mathbf{G}^H + (\text{tr}(\mathbf{R}_{\text{WW}})/E_L)\mathbf{I}_{NM_R})^{-1}$ , where  $\mathbf{R}_{\text{WW}} = E[\mathbf{W}\mathbf{W}^H]$ , and  $\text{tr}(\mathbf{A})$  denotes the trace of matrix  $\mathbf{A}$ . Although the MMSE linear precoder outperforms the ZF one at low signal-to-noise power ratio (SNR), the former approaches the latter at high SNR due to noise enhancement. In any event, a linear precoder may be hard to implement in OFDM as the reliable feedback of frequency-offset information to the transmitter is difficult, and hence, it will not be considered further.

#### B. Nonlinear Precoding

We now consider THP for ICI reduction in closed-loop OFDM systems. Direct application of conventional THP requires complete CSI at the transmitter, including channel-gain matrix  $\mathbf{H}$  and the ICI matrix  $\mathbf{S}$ , which is unrealistic. We first prove that the ICI coefficient matrix between the  $u$ th transmit and the  $v$ th receive antenna  $\mathbf{S}_{u,v}$  is approximately unitary.

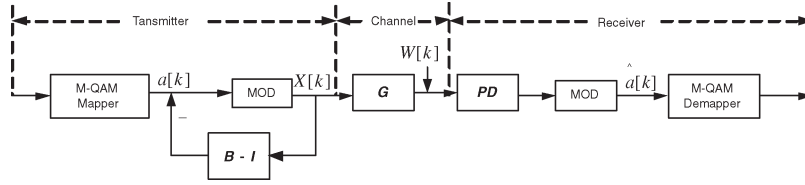


Fig. 2. Block diagram of THP in MIMO OFDM.

Consequently, the frequency offsets do not need to be fed back to the transmitter. The resulting nonlinear TH precoder reduces ICI in closed-loop SISO and MIMO OSTBC OFDM.

1) *Properties of the ICI Coefficient Matrix:* The following properties related to the ICI coefficient matrix on the  $\{u, v\}$ th channel (7) can be derived using (4).

- 1) Conjugate odd symmetry. The ICI coefficient matrix  $\mathbf{S}_{u,v}$  given by (7) is a function of the normalized frequency offset  $\varepsilon_{u,v}$ ,  $\mathbf{S}_{u,v} = \mathbf{S}_{u,v}(\varepsilon_{u,v})$ . An ICI coefficient matrix with a negative frequency offset can be obtained as the complex transpose of the matrix corresponding to a positive frequency offset with same magnitude, i.e.,  $\mathbf{S}_{u,v}^H(\varepsilon_{u,v}) = \mathbf{S}_{u,v}(-\varepsilon_{u,v})$ .
- 2) Unitary. The ICI coefficient matrix can be approximated as a unitary matrix, i.e.,  $\mathbf{S}_{u,v}\mathbf{S}_{u,v}^H = \mathbf{S}_{u,v}^H\mathbf{S}_{u,v} = \mathbf{I}_N$ . Therefore, the inverse of the interference matrix can be easily calculated by taking the conjugate transpose since  $\mathbf{S}_{u,v}^{-1} = \mathbf{S}_{u,v}^H$ .

A proof of these properties, which are used in the design of the nonlinear precoder, is in the Appendix.

2) *TH Precoding (THP):* Using these properties of the ICI coefficient matrix, we are now ready to design the nonlinear TH precoder. The whole setup (Fig. 2) involves a receiver-based feedforward matrix  $\mathbf{D}$  and a transmitter-based upper triangular feedback matrix  $\mathbf{B} = [B(i, j)]$ . Before discussing how to choose these matrices, let us briefly explain how the transmitter precoding operates.

Given the data carrying symbols  $a[k] \in \mathcal{A}$  (the  $M$ -ary constellation), the transmitted symbols  $X[k]$  are successively calculated via the feedback filter as

$$\begin{aligned} X[k] &= \text{MOD}_{2\sqrt{M}} \left\{ a[k] - \sum_{j=0}^{k-1} B(k, j)X[j] \right\} \\ &= a[k] + q[k] - \sum_{j=0}^{k-1} B(k, j)X[j]. \end{aligned} \quad (10)$$

The initial signal constellation  $\mathcal{A}$  is periodically expanded by the modulo arithmetic feedback structure at the transmitter. The modulo  $2\sqrt{M}$  operation can be considered as the signal-dependent addition  $a[k] + q[k]$ , where the real and imaginary parts of  $q[k]$  are the unique integer multiples of  $2\sqrt{M}$  for which  $\Re\{X[k]\} \in (-\sqrt{M}, \sqrt{M})$  and  $\Im\{X[k]\} \in (-\sqrt{M}, \sqrt{M})$ . Thus, the power of the precoded transmitted signals is bounded. If  $a[k]$  is an i.i.d. sequence with variance  $E_s$  and uniformly distributed on  $\mathcal{A}$ , then  $X[k]$  is also i.i.d. with variance  $(M/M - 1)E_s$  and uniformly distributed within bounds slightly larger than those of the initial constellation [11]. The modulo operation employed at the transmitter is nonlinear,

and a slicer at the receiver uses the same modulo operation in detecting the points of the initial constellation  $\mathcal{A}$ .

In conventional THP for the system described in (5), assuming that  $\mathbf{G}$  is a  $G \times G$  square matrix, the feedforward matrix is designed at the receiver by using a QR factorization of the overall channel matrix

$$\mathbf{G} = \mathbf{D}^H \mathbf{T} \quad (11)$$

where the feedforward matrix  $\mathbf{D}$  is a unitary matrix, and  $\mathbf{T} = [T(i, j)]$  is an upper triangular matrix [19]. Given the overall channel matrix  $\mathbf{G}$ , the feedback matrix under the ZF criterion becomes  $\mathbf{B} = \mathbf{P}\mathbf{T}$ , where the scaling matrix  $\mathbf{P} = \text{diag}[T^{-1}(1, 1), \dots, T^{-1}(G, G)]$  keeps the average transmit power constant. This conventional THP design requires that both the frequency offset and channel response are available at the transmitter, which is undesirable. Exploiting the properties of the ICI coefficient matrix, we propose a TH precoder using only partial CSI at the transmitter.

a) *SISO OFDM:* When we only have one transmit antenna and one receive antenna, the overall channel matrix  $\mathbf{G}$  is an  $N \times N$  matrix. As in (11), we need a QR factorization of the overall channel matrix  $\mathbf{G}$ . However,  $\mathbf{G} = \mathbf{S}\mathbf{H}$  can be considered as a QR factorization because the ICI coefficient matrix  $\mathbf{S}$  is an  $N \times N$  unitary matrix, and the channel-gain matrix  $\mathbf{H}$  is  $N \times N$  diagonal. The feedback matrix thus is  $\mathbf{B} = \mathbf{P}\mathbf{H}$ , where the scaling matrix  $\mathbf{P} = \text{diag}[T^{-1}(1, 1) \dots T^{-1}(N, N)]$ ;  $T(m, m)$  is the  $m$ th main-diagonal entry of the matrix  $\mathbf{T}$ , which is obtained by the Cholesky factorization  $\mathbf{H}\mathbf{H}^H = \mathbf{T}\mathbf{T}^H$ . Regardless of the modulo reduction, the average power of the transmitted signal  $\mathbf{X} = \mathbf{B}^{-1}\mathbf{A}$  can be given as

$$\begin{aligned} E_X &= E[\mathbf{H}^{-1}\mathbf{P}^{-1}\mathbf{A}\mathbf{A}^H\mathbf{P}^{-H}\mathbf{H}^{-H}] \\ &= E_s E[\mathbf{H}^{-1}\mathbf{T}\mathbf{T}^H\mathbf{H}^{-H}] = E_s \mathbf{I}. \end{aligned} \quad (12)$$

At the receiver, the feedforward matrix is  $\mathbf{D} = \mathbf{S}^H$ . Note that if we directly factorize the overall channel matrix  $\mathbf{G}$ , which decomposes  $\mathbf{G}$  as a product of a unitary matrix and an upper triangular matrix, we have to know both channel response and frequency offset at the transmitter. Since the ICI coefficient matrix  $\mathbf{S}$  is unitary and the  $\mathbf{H}$  is a diagonal matrix in the SISO case,  $\mathbf{G} = \mathbf{S}\mathbf{H}$  can be considered as QR factorization, i.e., we do not need to factorize the overall channel matrix. The channel-gain matrix  $\mathbf{H}$  becomes the feedback matrix at the transmitter, and  $\mathbf{S}^H$  becomes the feedforward matrix at the receiver. Hence, the knowledge of frequency offset at the transmitter is not necessary.

Since the linear predistortion via  $\mathbf{B}^{-1}$  equalizes the cascade  $\mathbf{G}\mathbf{P}\mathbf{D}$ , after the unitary prefilter  $\mathbf{D}$  at the receiver, the data symbols  $a[k]$  are corrupted by an additive noise as

$Y[k] = a[k] + q[k] + W'[k]$ , where  $W'[k]$  is the  $k$ th entry of filtered noise vector  $\mathbf{W}' = \mathbf{P}\mathbf{D}\mathbf{W}$  with individual variance  $\sigma_{W'_k}^2 = \sigma_W^2 T^{-2}(k, k)$ . Since the modulo arithmetic device at the receiver applies the same modulo operation as that at the transmitter, unique estimates of the data symbols are generated. Consequently, after discarding the modulo congruence, the proposed precoder completely cancels ICI.

*b) MIMO OFDM:* For the MIMO case, we have the  $\text{NM}_R \times \text{NM}_T$  overall channel matrix  $\mathbf{G}$ , the  $\text{NM}_R \times \text{NM}_R \text{M}_T$  ICI matrix  $\mathbf{S}$  (6), and the  $\text{NM}_R \text{M}_T \times \text{NM}_T$  channel-gain matrix  $\mathbf{H}$  (8). For convenience of signal detection, we assume that  $M_R \geq M_T$ . In the most general case, each transmit–receive antenna pair may have a different frequency offset if the collocated antennas do not share the same oscillator. In this section, we consider the case of  $M_R$  different frequency offsets, i.e., for the  $v$ th receive antenna,  $\varepsilon_{1,v} = \varepsilon_{2,v} = \dots = \varepsilon_{M_T,v} = \varepsilon_v$ , and  $\varepsilon_v \neq \varepsilon_{v'}, \forall v \neq v'$ .

Since the frequency offset  $\varepsilon_{u,v}, \forall u$ , is identical to  $\varepsilon_v$ ,  $\mathbf{S}_{1,v} = \dots = \mathbf{S}_{M_T,v} = \mathcal{S}_v$ ; and  $\mathcal{S}_v$  is an  $N \times N$  unitary matrix. The overall channel matrix  $\mathbf{G}$  can be rewritten as

$$\mathbf{G} = \mathcal{S}\mathcal{H} \quad (13)$$

where the  $\text{NM}_R \times \text{NM}_T$  channel-gain matrix is

$$\mathcal{H} = \begin{bmatrix} \mathbf{H}_{1,1} & \cdots & \mathbf{H}_{M_T,1} \\ \vdots & \ddots & \vdots \\ \mathbf{H}_{1,M_R} & \cdots & \mathbf{H}_{M_T,M_R} \end{bmatrix} \quad (14)$$

and the  $\text{NM}_R \times \text{NM}_R$  ICI matrix is

$$\mathcal{S} = \text{diag}[\mathcal{S}_1 \cdots \mathcal{S}_{M_R}]. \quad (15)$$

Since the  $\mathcal{S}_v$  is unitary,  $\mathcal{S}$  is also a unitary matrix.

Instead of factorization of the overall channel matrix  $\mathbf{G}$ , we design the filters of THP by QR factorization of the channel-gain matrix  $\mathcal{H}$

$$\mathcal{H} = \mathbf{F}^H \mathbf{T} \quad (16)$$

with an  $\text{NM}_R \times \text{NM}_R$  unitary matrix  $\mathbf{F}$  and an  $\text{NM}_R \times \text{NM}_T$  upper triangular matrix  $\mathbf{T}$

$$\mathbf{T} = \begin{bmatrix} \check{\mathbf{T}} \\ \mathbf{0}_{N(M_R-M_T) \times \text{NM}_T} \end{bmatrix} \quad (17)$$

where  $\check{\mathbf{T}}$  is an  $\text{NM}_T \times \text{NM}_T$  upper triangular matrix. We design the feedforward matrix as  $\mathbf{D} = \mathbf{F}\mathcal{S}^H$  so that  $\mathbf{G} = \mathbf{D}^H \mathbf{T} = \mathcal{S}\mathbf{F}^H \mathbf{T} = \mathcal{S}\mathcal{H}$ . Since both  $\mathbf{F}$  and  $\mathcal{S}$  are unitary, the feedforward matrix  $\mathbf{D}$  is unitary as well. The feedback filter is set as an  $\text{NM}_T \times \text{NM}_T$  matrix  $\mathbf{B} = \check{\mathbf{P}}\check{\mathbf{T}}$ , where the  $\text{NM}_T \times \text{NM}_T$  diagonal matrix  $\check{\mathbf{P}}$  satisfies  $\text{E}[\check{\mathbf{T}}^H \check{\mathbf{P}}^H \check{\mathbf{P}} \check{\mathbf{T}}] = \mathbf{I}$ . At the receiver, the scaling matrix is  $\mathbf{P} = [\check{\mathbf{P}} \quad \mathbf{0}_{\text{NM}_T \times N(M_R-M_T)}]$ . The received signals at the output of the slicer can be given as

$$\hat{\mathbf{A}} = \mathbf{P}\mathbf{D}\mathbf{G}\mathbf{B}^{-1}\mathbf{A} + \mathbf{P}\mathbf{D}\mathbf{W} = \Psi\mathbf{A} + \mathbf{W}' \quad (18)$$

where  $\Psi = \mathbf{P}\mathbf{D}\mathbf{G}\mathbf{B}^{-1} = \mathbf{P}\mathbf{D}\mathcal{D}^H\check{\mathbf{P}}^\dagger$  is approximately an  $\text{NM}_T \times \text{NM}_T$  identity matrix, if perfect channel-gain matrix  $\mathcal{H}$  is known at the transmitter.

The proposed TH precoder for both SISO and MIMO OFDM systems, not needing the knowledge of frequency offsets at the transmitter, reduces information load in the feedback channel and avoids the possible frequency-offset transmitter mismatch due to feedback errors and delay in practical implementation. With perfect information of channel impulse response at the transmitter and knowledge of frequency offset at the receiver, our proposed THP outperforms than linear precoding. Furthermore, because the feedback filter is moved to the transmitter in the TH precoder, the error propagation, which inevitably degrades BER in DFE, is avoided. Therefore, lower BER can be expected for THP.

*3) TH Precoder for Alamouti-Coded OFDM:* We next consider the important special case of OSTBC, the Alamouti code [20] for 2 transmit antennas and multiple receive antennas. The Alamouti code is used in space–time transmit diversity, which has been adopted by the 3GPP because it maximizes diversity gain [3], [4]. We also generalize the proposed precoder design for an arbitrary number of transmit antennas.

The Alamouti code can be described by a  $2 \times 2$  code matrix  $\mathbf{C} = \begin{bmatrix} c_1 & -c_2^* \\ c_2 & c_1^* \end{bmatrix}$ , i.e., two symbols  $c_1$  and  $c_2$  and their conjugates are transmitted over two time slots [20]. At the first time slot, the  $c_1$  and  $c_2$  are transmitted from the antenna 1 and 2, respectively; during the next symbol period,  $-c_2^*$  is transmitted from the antenna 1, and  $c_1^*$  is from the antenna 2. Consequently, in Alamouti-coded OFDM with proposed THP, the output sequence of the feedforward filter can be given as

$$\begin{bmatrix} \tilde{\mathbf{A}}_1 & \tilde{\mathbf{A}}_3 \\ \tilde{\mathbf{A}}_2 & \tilde{\mathbf{A}}_4 \end{bmatrix} = \Psi \begin{bmatrix} \mathbf{A}_1 & -\mathbf{A}_2^* \\ \mathbf{A}_2 & \mathbf{A}_1^* \end{bmatrix} + \mathbf{W}' \quad (19)$$

where the  $2N \times 2N$  matrix  $\Psi = \begin{bmatrix} \tilde{\mathbf{I}}_N & 0 \\ 0 & \tilde{\mathbf{I}}_N \end{bmatrix}$  as in (18);  $\tilde{\mathbf{I}}_N$  is approximately an identity matrix. The vectors  $\mathbf{A}_1 = [a_1[0] \cdots a_1[N-1]]^T$  and  $\mathbf{A}_2 = [a_2[0] \cdots a_2[N-1]]^T$  are transmitted over the first and second antenna at the first time slot, respectively; and the  $-\mathbf{A}_2^*$  and  $\mathbf{A}_1^*$  are transmitted in sequence in consecutive time slots. The received signal matrices can be represented as

$$\begin{aligned} \hat{\mathbf{A}}_1 &= \tilde{\mathbf{A}}_1 + \tilde{\mathbf{A}}_4^* = 2\mathbf{A}_1 + \mathbf{W}'_1 + \mathbf{W}'_4^* \\ \hat{\mathbf{A}}_2 &= \tilde{\mathbf{A}}_2 - \tilde{\mathbf{A}}_3^* = 2\mathbf{A}_2 + \mathbf{W}'_2 - \mathbf{W}'_3^* \end{aligned} \quad (20)$$

*4) TH Precoder for Generalized OSTBC OFDM:* An  $M_T \times T$  code matrix for generalized orthogonal STBC [21] obeys

$$\mathbf{C}\mathbf{C}^H = \left( \sum_{n=1}^{N_c} |c_n|^2 \right) \mathbf{I} \quad (21)$$

for all complex codewords  $c_n$ , where  $N_c$  represents the number of symbols transmitted over the  $T$  time slots. The rate is defined as  $N_c/T$ . Complex orthogonal designs with full rate do not exist for more than two antennas. Complex orthogonal designs with 3/4 rate for three and four transmit antennas and 1/2 rate for arbitrary number of transmit antennas are described in [21].

When  $M_T > 2$ , the received signals are

$$\begin{bmatrix} \tilde{\mathbf{A}}_{11} & \cdots & \tilde{\mathbf{A}}_{1T} \\ \vdots & \ddots & \vdots \\ \tilde{\mathbf{A}}_{M_T 1} & \cdots & \tilde{\mathbf{A}}_{M_T T} \end{bmatrix} = \begin{bmatrix} \tilde{\mathbf{I}}_N & \cdots & \mathbf{0} \\ \vdots & \ddots & \vdots \\ \mathbf{0} & \cdots & \tilde{\mathbf{I}}_N \end{bmatrix} \mathbf{C} + \mathbf{W}' \quad (22)$$

where the element in the  $NM_T \times T$  code matrix  $\mathbf{C}$  is a  $M_T \times 1$  transmitted OFDM symbol vector. For instance, for 1/2 rate OSTBC OFDM with 4 transmit antennas, the input matrices for ML-detector can be given by

$$\begin{aligned} \hat{\mathbf{A}}_1 &= \tilde{\mathbf{A}}_{11} + \tilde{\mathbf{A}}_{22} + \tilde{\mathbf{A}}_{33} + \tilde{\mathbf{A}}_{44} - \tilde{\mathbf{A}}_{15}^* - \tilde{\mathbf{A}}_{26}^* - \tilde{\mathbf{A}}_{37}^* - \tilde{\mathbf{A}}_{48}^* \\ \hat{\mathbf{A}}_2 &= \tilde{\mathbf{A}}_{21} - \tilde{\mathbf{A}}_{12} + \tilde{\mathbf{A}}_{34} - \tilde{\mathbf{A}}_{43} + \tilde{\mathbf{A}}_{25}^* - \tilde{\mathbf{A}}_{16}^* + \tilde{\mathbf{A}}_{38}^* - \tilde{\mathbf{A}}_{47}^* \\ \hat{\mathbf{A}}_3 &= \tilde{\mathbf{A}}_{31} - \tilde{\mathbf{A}}_{13} + \tilde{\mathbf{A}}_{24} - \tilde{\mathbf{A}}_{42} + \tilde{\mathbf{A}}_{35}^* - \tilde{\mathbf{A}}_{17}^* + \tilde{\mathbf{A}}_{28}^* - \tilde{\mathbf{A}}_{46}^* \\ \hat{\mathbf{A}}_4 &= \tilde{\mathbf{A}}_{41} - \tilde{\mathbf{A}}_{14} + \tilde{\mathbf{A}}_{23} - \tilde{\mathbf{A}}_{32} + \tilde{\mathbf{A}}_{45}^* - \tilde{\mathbf{A}}_{18}^* + \tilde{\mathbf{A}}_{27}^* - \tilde{\mathbf{A}}_{36}^*. \end{aligned} \quad (23)$$

5) *TH Precoder for  $M_T \times M_R$  Distinct Frequency Offsets:* In this section, we consider the most general case where we have  $M_T \times M_R$  different frequency offsets. When the frequency offsets are different between different transmit-receive antenna pairs, the ICI coefficient matrix  $\mathbf{S}_{u,v} \neq \mathbf{S}_{u',v'}, \forall u \neq u', v \neq v'$ , and the ICI matrix  $\mathbf{S}$  in (6) is not unitary. The feedforward filter  $\mathbf{D} = \mathbf{F}\mathbf{S}^H$  is thus not unitary as well, where  $\mathbf{F}$  is obtained by QR factorization of the channel-gain matrix  $\mathbf{H}$  in (8). After the feedforward filter, the noise variance matrix is  $\mathbf{R}_{W'W'} = \mathbf{PDR}_{WW}\mathbf{D}^H\mathbf{P}^H$ , which is not a diagonal matrix, i.e., the noise is correlated. A whitening processor is thus needed for the ML detection. A whitening filter as in [22] can be used to whiten the colored noise and reduce computational complexity of ML decoding. This whitening filter is equivalent to a weight matrix for MMSE restoration of the desired signal followed by whitening of the residual interference and noise. An ML detection in addition to a slicer generates the estimate of the transmitted symbol  $\hat{a}[k]$ .

### C. Effect of Mismatch on Precoding Performance

If ideal feedback and precise channel estimates exist, closed-loop systems offer a substantial advantage over their open-loop counterparts. However, erroneous estimates and/or imperfect feedback results in transmitter channel mismatch, i.e., the channel information that is available at the transmitter differs from the actual channel at the time of transmission due to imperfect estimation, feedback delay, and errors. We consider two cases of channel mismatch. In the first case, the receiver knows  $\mathbf{H}$  perfectly, but the transmitter has imperfect channel matrix  $\hat{\mathbf{H}}$  because of feedback delay or noise. In the second case, the receiver has the imperfect channel estimate  $\mathbf{H}_R$ , while the transmitter has  $\mathbf{H}_T$ , which is a noise-corrupted version of  $\mathbf{H}_R$  because of imperfect feedback. The  $\mathbf{H}_T$  is unknown at the receiver. Since we do not need to send frequency offsets back to the transmitter, the frequency-offset transmitter mismatch is not considered here. The impact of frequency-offset mismatch in conventional THP is shown in the simulation part.

Without the proposed TH precoder, the SNR of an OFDM system in the presence of frequency offset can be given as [23]

$$\text{SNR}_{u,v} = \frac{\text{sinc}^2(\varepsilon_{u,v})\sigma_{H_{u,v}}^2 E_s}{[1 - \text{sinc}^2(\varepsilon_{u,v})]\sigma_{H_{u,v}}^2 E_s + \sigma_W^2} \quad (24)$$

where  $\sigma_{H_{u,v}}^2 = E[|H_{u,v}[k]|^2], \forall k$ . When  $\varepsilon_{u,v} = 0$ , the SNR converts to  $\text{SNR}_{u,v}^0 = \sigma_{H_{u,v}}^2 E_s / \sigma_W^2$ . With the TH precoder, if the channel-gain matrix  $\mathbf{H}$  is perfectly known at both transmitter and receiver, the SNR for the  $k$ th subcarrier can be given as  $\text{SNR}_{u,v}^0 = \sigma_{H_{u,v}}^2 E_s / \sigma_{W'}^2[k]$ .

Let  $\hat{\mathbf{B}}$  and  $\hat{\mathbf{D}}$  correspond to the feedback and feedforward filters of THP designed for  $\hat{\mathbf{H}} \neq \mathbf{H}$ . The  $\hat{\mathbf{D}}\mathbf{G} - \hat{\mathbf{B}}$  has a term  $g_0[k]$  at the zero-lag tap for the  $k$ th subcarrier. The output SNR is

$$\text{SNR}_{u,v}[k] = \frac{g_0^2[k]E_s}{\sigma_{\text{ICI}_{u,v}}^2[k] + \sigma_{W'}^2[k]}. \quad (25)$$

The residual ICI limits the output SNR and degrades the system performance.

1) *First Case:* In the first case, the receiver has perfect knowledge of the channel  $\mathbf{H}$ , but the transmitter has an incorrect estimate  $\hat{\mathbf{H}}$  because of errors or delay in the feedback link. The received signals are

$$\hat{\mathbf{A}} = \mathbf{P}\hat{\mathbf{D}}\hat{\mathbf{G}}\hat{\mathbf{B}}^{-1}\mathbf{A} + \mathbf{W}' = \hat{\Psi}\mathbf{A} + \mathbf{W}' \quad (26)$$

where  $\hat{\Psi} = \hat{\mathbf{P}}\hat{\mathbf{T}}\hat{\mathbf{B}}^{-1} = \hat{\mathbf{B}}\hat{\mathbf{B}}^{-1}$ . Obviously,  $\hat{\Psi}$  is not an identity matrix as  $\Psi$  in (18). Generally,  $\hat{\mathbf{B}}\hat{\mathbf{B}}^{-1}$  is not a diagonal matrix and introduces residual ICI. For SISO systems, since  $\mathbf{B}$  is a diagonal matrix,  $\hat{\mathbf{B}}\hat{\mathbf{B}}^{-1}$  is also a diagonal matrix. Hence, in a SISO system, if both  $\mathbf{S}$  and  $\mathbf{H}$  are perfectly known at the receiver, errors in  $\hat{\mathbf{H}}$  in our precoder only results in signal power loss but no residual ICI.

2) *Second Case:* In the second case of channel information mismatch, the receiver has an imperfect frequency-offset estimate  $\hat{\mathbf{S}}$  and the incorrect channel-gain estimate  $\mathbf{H}_R$ , while the transmitter has  $\mathbf{H}_T$ , which is the noise-corrupted version of  $\mathbf{H}_R$ . The  $\mathbf{H}_T$  is unknown at the receiver, and  $\mathbf{H}_T \neq \mathbf{H}_R \neq \mathbf{H}$ . At the transmitter,  $\hat{\mathbf{B}}$  is constructed from  $\mathbf{H}_T$  and at the receiver  $\hat{\mathbf{D}}$  from  $\mathbf{H}_R$  and  $\hat{\mathbf{S}}$ . This leads to a nonidentity matrix  $\hat{\Psi} = \hat{\mathbf{P}}\hat{\mathbf{D}}\hat{\mathbf{G}}\hat{\mathbf{B}}^{-1}$ . With the proposed THP in Alamouti-coded OFDM, the received signals in (19) become

$$\hat{\mathbf{A}} = \hat{\Psi}\mathbf{A} + \mathbf{W}' = \begin{bmatrix} \hat{\Psi}_1 & \hat{\Psi}_2 \\ \hat{\Psi}_3 & \hat{\Psi}_4 \end{bmatrix} \mathbf{A} + \mathbf{W}' \quad (27)$$

where the  $N \times N$  matrices  $\hat{\Psi}_1$  and  $\hat{\Psi}_4$  are not approximately identity, and  $\hat{\Psi}_2$  and  $\hat{\Psi}_3$  are not zero matrices. The signal matrices for the ML detection are hence given by

$$\begin{aligned} \hat{\mathbf{A}}_1 &= \hat{\Psi}_1 \mathbf{A}_1 + \hat{\Psi}_4^* \mathbf{A}_1 + \hat{\Psi}_2 \mathbf{A}_2 - \hat{\Psi}_3^* \mathbf{A}_2 + \mathbf{W}'_1 + \mathbf{W}'_4^* \\ \hat{\mathbf{A}}_2 &= \hat{\Psi}_1^* \mathbf{A}_2 + \hat{\Psi}_4 \mathbf{A}_2 + \hat{\Psi}_3 \mathbf{A}_1 - \hat{\Psi}_2^* \mathbf{A}_1 + \mathbf{W}'_2 - \mathbf{W}'_3^*. \end{aligned} \quad (28)$$

Clearly, cochannel interference (CCI) and residual ICI are introduced to the combined signals. In SISO systems, no CCI

occurs, however, since  $\hat{\mathbf{D}}\hat{\mathbf{D}}^H \neq \mathbf{I}_N$  and  $\mathbf{T}\hat{\mathbf{T}}^{-1} \neq \mathbf{I}_N$ , residual ICI is still introduced.

#### IV. CORRELATED SPATIAL CHANNELS

The MIMO channel with spatial correlations of its gains is studied in this section. The correlated channel model builds on previous work reported in [24] and [25]. For the sake of simplicity, we assume a uniform linear array at the transmitter and receiver with identical antenna elements. The channel matrix  $\tilde{\mathbf{H}}$  is assumed to be zero-mean (Rayleigh fading) circularly symmetric complex Gaussian distributed with a separable spatial correlation function.

For a frequency-selective channel with  $M_T$  transmit and  $M_R$  receive antennas, the  $l$ th tap gain can be represented by an  $M_R \times M_T$  matrix  $\mathbf{h}(l)$ ,  $\forall l$ . A channel-gain vector from all the taps is  $\tilde{\mathbf{h}} = [\text{vec}(\mathbf{h}(0))^T \cdots \text{vec}(\mathbf{h}(L-1))^T]^T$ , where  $\text{vec}(\cdot)$  denotes the vectorization operator [24]. According to the model in [25], the spatial gain correlation matrix can be represented by

$$\mathbf{R} = E[\tilde{\mathbf{h}}\tilde{\mathbf{h}}^H] = \mathbf{R}_P \otimes \mathbf{R}_T^T \otimes \mathbf{R}_R \quad (29)$$

where  $\mathbf{R}_P$  is the  $L \times L$  path correlation matrix; if the paths between each transmit–receive antenna pair are uncorrelated, the  $\mathbf{R}_P = \text{diag}[\sigma_0^2 \cdots \sigma_{L-1}^2]$  is only determined by the power delay profiles. The  $\mathbf{R}_T$  and  $\mathbf{R}_R$  are the transmit and receive antenna correlation matrices. From [24], the entries of  $\mathbf{R}_T$  and  $\mathbf{R}_R$  are

$$\begin{aligned} R_T(m, n) &= J_0 \left( 2\pi\Delta |m - n| \frac{d_T}{\lambda} \right) \\ R_R(m, n) &= J_0 \left( 2\pi |m - n| \frac{d_R}{\lambda} \right) \end{aligned} \quad (30)$$

where  $J_0$  is zero-order Bessel function of the first kind, and  $\Delta = \arcsin(r/d)$  is the angle spread [24]; the  $r$  is the radius of the scatter ring, and the  $d$  is the distance between transmit and receive antennas. The  $\lambda = c/f_c$  is the wavelength of a narrowband signal with center frequency  $f_c$ . The antennas at the transmitter and receiver are spaced by  $d_T$  and  $d_R$ , respectively. The tap gain vector therefore can be obtained as

$$\text{vec}(\mathbf{h}(l)) = [\mathbf{R}_T^T \otimes \mathbf{R}_R]^{1/2} \text{vec}(\mathbf{h}_w(l)) \quad (31)$$

where  $\text{vec}(\mathbf{h}_w(l))$  is an  $M_R M_T$ -dimensional vector of i.i.d. zero mean complex Gaussian random variables with variance  $\sigma_l^2$ .

Using  $\mathbf{h}(l)$  in (31),  $\forall l$ , the spatially correlated channel-gain matrix  $\tilde{\mathbf{H}}$  can be constructed as the same structure as  $\mathbf{H}$  (8) or  $\mathcal{H}$  (14). The proposed nonlinear TH precoder can also be used in MIMO OFDM when the spatial channels are correlated. With known fading correlations at the transmitter, we do QR factorization of  $\tilde{\mathbf{H}}$  instead of  $\mathcal{H}$  or  $\mathbf{H}$ . The design of feedback and feedforward filters is the same as that described in Section III.

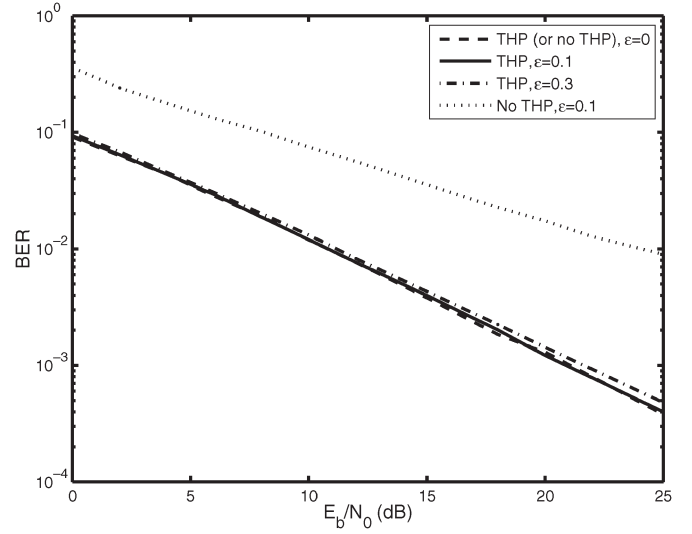


Fig. 3. BER with THP as a function of the SNR for different values of the normalized frequency offset for closed-loop SISO QPSK-OFDM ( $N = 64$ ), with perfect channel-gain matrix at both the transmitter and the receiver.

#### V. SIMULATION RESULTS

In this section, simulation results show how the proposed TH precoder suppresses ICI in OFDM. The vehicular B channel specified by ITU-R M. 1225 [26] is used where the channel taps are zero-mean complex Gaussian random processes with variances of  $-4.9$ ,  $-2.4$ ,  $-15.2$ ,  $-12.4$ ,  $-27.6$ , and  $-18.4$  dB relative to the total power normalized to unity. For many wireless systems, the multipath channels fade slowly. As an example, for wireless local area network employing a relatively high carrier frequency of 5 GHz [27], even at a mobile speed as high as 60 km/h, which leads to a relatively high value of the maximum Doppler shift of 278 Hz, the corresponding normalized maximum Doppler shift is only roughly 0.001, when the symbol period is 3.2  $\mu\text{s}$  and  $N = 64$  (parameters of the simulated 20-MHz OFDM system). The channel gains can thus be assumed constant over several OFDM symbol intervals.

##### A. SISO OFDM

Fig. 3 gives the BER as a function of SNR for different values of the normalized frequency offset in SISO OFDM with perfect channel knowledge at both the transmitter and the receiver. The performance of OFDM without precoding is shown as a reference. The proposed THP clearly reduces ICI significantly. For instance, with a normalized frequency offset of 10%, THP-OFDM has almost the same BER as an OFDM system in the absence of frequency offset, i.e., the ICI has been cancelled almost completely.

Fig. 4 presents BER of THP-OFDM when the receiver has perfect knowledge of channel-gain matrix  $\mathbf{H}$ , while the transmitter has an imperfect channel matrix  $\tilde{\mathbf{H}}$  due to the feedback channel noise. Since the feedback channel bandwidth is usually much smaller than the downlink traffic channel capacity, we assume the noise variance of the feedback link to be  $\sigma_F^2 = \sigma_W^2/100$ . The frequency offset is perfectly estimated at the receiver. The BER of OFDM with conventional THP is also shown as a reference in Fig. 4. In that reference case,

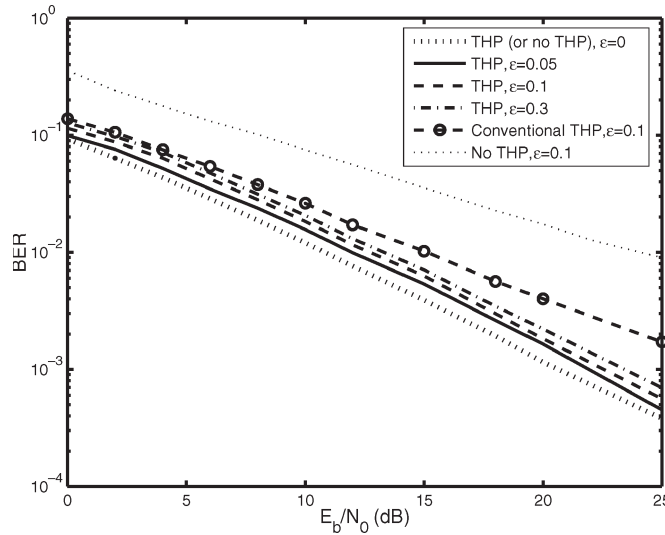


Fig. 4. BER with THP as a function of the SNR for different values of the normalized frequency offset for closed-loop SISO QPSK-OFDM ( $N = 64$ ) with perfect channel-gain matrix at the receiver and inaccurate channel-gain matrix at the transmitter.

conventional THP uses a noise-corrupted frequency offset at the transmitter, which leads to serious ICI residuals. Our precoder minimizes the BER degradation by avoiding such frequency-offset mismatch.

In Fig. 5, we assume that at the receiver, the channel-gain matrix estimate  $\mathbf{H}_R$  is imperfect, while the transmitter uses a channel-gain matrix estimate corrupted further by feedback errors. The frequency offset is also estimated at the receiver with reasonable quality. The estimation schemes used are described in [28] and the references therein. We assume that the channel-gain matrix  $\mathbf{H}$  does not change within two consecutive OFDM symbol periods. At SNR = 20 dB, with the frequency-offset estimation algorithm described in [28], the average normalized mse of the frequency-offset estimate is  $1.44 \times 10^{-3}$  for 10% normalized frequency offset and  $6.30 \times 10^{-3}$  for 30% normalized frequency offset. With the estimated frequency offset assumed constant over at least one OFDM symbol, the channel gains are estimated using pilot symbols as in [29], where pilot symbols are multiplexed with the OFDM blocks in the time domain to enable channel estimation. In order to guarantee reasonable performance of the channel estimator, every OFDM symbol is followed by a pilot block of length  $2N_{CP}$ , where  $N_{CP}$  is the length of cyclic prefix. In our case,  $N = 64$ , and  $N_{CP} = 16$ . The throughput loss incurred due to the pilot blocks is  $2N_{CP}/(N + N_{CP})$ . For a given data rate, it is possible that  $N \gg N_{CP}$  if the number of subcarriers is large. In this case, the throughput loss will be small. With the estimation algorithm used, at SNR = 20 dB, the average normalized mse of the channel-gain estimates is around 0.036 with a normalized frequency offset of 10% and 0.047 with a normalized frequency offset of 30%. The value of mse decreases as SNR increases. The channel-gain estimates are conveyed to the transmitter via a noisy feedback link with noise variance  $\sigma_F^2 = \sigma_W^2/100$ . In OFDM with conventional THP, the estimated frequency offset has to be sent back, which introduces further mismatch due to errors in frequency-offset information available at the

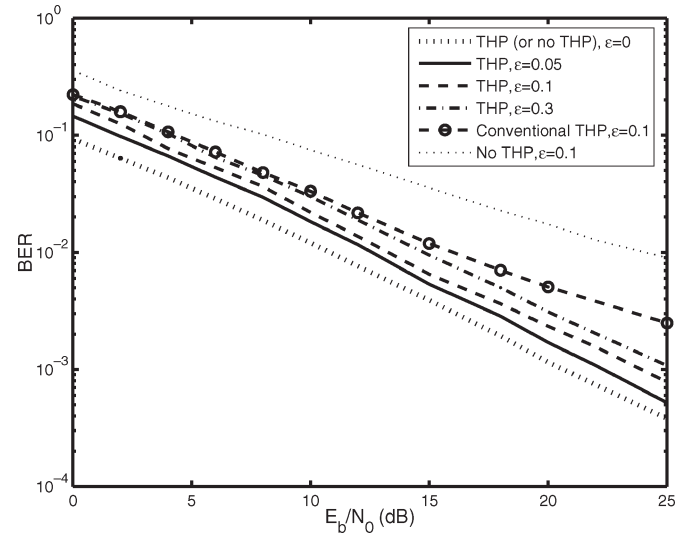


Fig. 5. BER with THP as a function of the SNR for different values of the normalized frequency offset for SISO QPSK-OFDM ( $N = 64$ ) with inaccurate channel-gain matrices used at both transmitter and receiver.

transmitter and may result in severe performance loss. In our precoder, however, frequency-offset information is not needed at the transmitter, and the errors in channel estimates only lead to slight BER degradations.

## B. MIMO OFDM

The performance of Alamouti-coded OFDM with THP is discussed in this section. For simplicity, we assume that both the transmitter and the receiver have the perfect channel-gain matrix  $\mathbf{H}$  information, and the receiver has perfect knowledge of frequency offsets. We consider a general case where we have  $M_R$  different frequency offsets. The values of normalized frequency offsets are assumed to be uniformly distributed in two intervals  $\mathbb{I} = (0, 0.1]$  and  $\mathbb{III} = (0.1, 0.3]$ .

1) *Uncorrelated Spatial Channels*: In Fig. 6, the spatial channels between different transmit and receive antenna pairs are uncorrelated. We show the BER performance of  $2 \times 2$  and  $2 \times 4$  Alamouti-coded OFDM with THP in the presence of  $M_R$  different frequency offsets. The BER of  $2 \times 2$  Alamouti-coded OFDM without THP when  $\varepsilon_v \in \mathbb{I}$  is provided as a reference. Just as for SISO OFDM, our TH precoder reduces ICI significantly in this case. When the normalized frequency offsets  $\varepsilon_v \in \mathbb{I}$ , the ICI can be cancelled almost completely. In addition, a  $2 \times 4$  OFDM system achieves better performance due to higher diversity order. Our precoder also can be used for the worst case when the frequency offsets corresponding to different antenna pairs are different. The maximum possible number of distinct frequency-offset values is  $M_T \times M_R$ . Our precoder thus leads to savings of feedback capacity necessary to transmit information on  $M_T \times M_R$  frequency offsets. Using the prewhitening filter as in [22], the proposed THP for this case has a slight degradation compared with the case of  $M_R$  different frequency offsets.

2) *Correlated Spatial Channels*: In Fig. 7, we consider  $2 \times 2$  OFDM with  $M_R$  different frequency offsets. The angle spread  $\Delta$  in (30) is set to 0.1. The distances between the



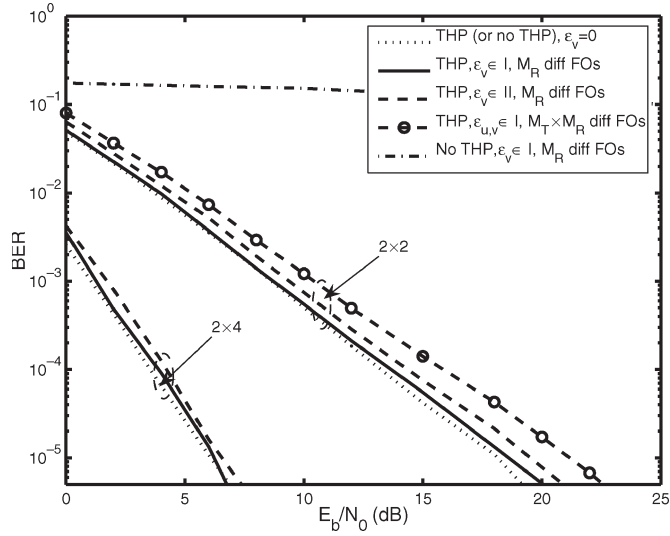


Fig. 6. BER as a function of the SNR for different values of the normalized frequency offset for  $2 \times 2$  and  $2 \times 4$  Alamouti-coded OFDM ( $N = 64$ ) with THP; perfect channel-gain estimates and uncorrelated spatial channels.

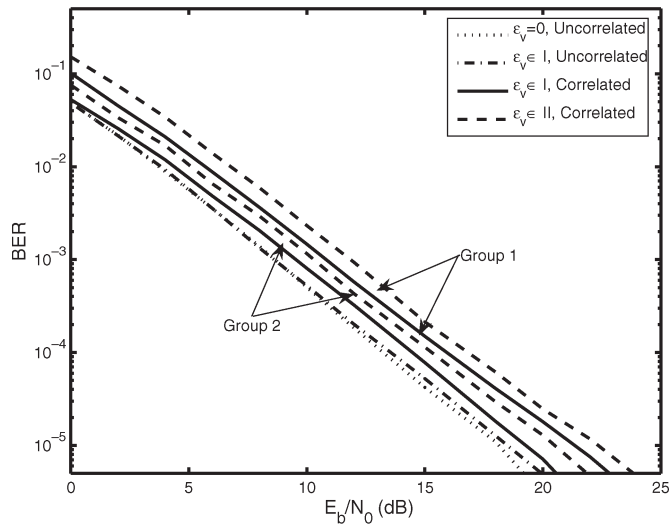


Fig. 7. BER as a function of the SNR for different values of the normalized frequency offset for  $2 \times 2$  Alamouti-coded OFDM ( $N = 64$ ) with THP and correlated spatial channels. The fading correlations are unknown, and  $\rho = 0.3$  in Group 1. The fading correlations are known at the transmitter, and  $\rho = 0.7$  in Group 2.

antennas are assumed to be less than  $\lambda/2$ , which causes sufficient fading correlations. The correlation coefficient  $\rho$  is defined as  $\rho = \max[r(m, n)/\sqrt{r(m, m)r(n, n)}]$ ,  $\forall m \neq n$ , where  $r(m, n)$  is the  $\{m, n\}$ th entry of  $[\mathbf{R}_T^T \otimes \mathbf{R}_R]^{1/2}$  in (31).

Fig. 7 shows two groups of BER curves for two cases of correlations. In the first group,  $\rho = 0.3$ , and the fading correlations are unknown at the transmitter. In the second group,  $\rho = 0.7$ , and the fading correlations are known at the transmitter. With the known fading correlations at the transmitter, we QR factorize  $\tilde{\mathbf{H}}$  instead of  $\mathcal{H}$ . The BERs of  $2 \times 2$  Alamouti-coded OFDM with zero frequency offset and Alamouti-coded THP-OFDM with  $\varepsilon_v \in \mathbb{I}$  in uncorrelated spatial fading channels are given as references. The fading correlations degrade the MIMO OFDM performance. However, THP reduces the effect

of fading correlations, and the BER loss is marginal when the fading correlations are known at the transmitter.

## VI. CONCLUSION

We have derived a nonlinear TH precoder for ICI reduction in closed-loop SISO and MIMO OFDM. We have shown that the ICI coefficient matrix is approximately unitary and used this property to design the precoder for ICI suppression with only partial CSI available at the transmitter, not including the knowledge of frequency offsets. Since frequency offsets do not necessary have to be fed back to the transmitter, our approach reduces the feedback load in closed-loop MIMO OFDM systems and avoids the detrimental effect of frequency-offset mismatch due to imperfect feedback. The degradation due to frequency offset can be significantly reduced by the proposed nonlinear TH precoder in both SISO and MIMO OFDM. For spatially correlated channels, an OSTBC MIMO OFDM system with our THP performs with negligible BER-performance loss.

## APPENDIX

For simplicity, in the following proof, we omit the subscript  $\{u, v\}$ .

*Proof of conjugate odd symmetry property of  $\mathbf{S}$ :* As  $N \gg 1$ , for  $1 \leq k < N/2$  and  $k \gg \varepsilon$ , we have

$$\begin{aligned} S[k] &\approx \frac{\sin \pi(\varepsilon + k)}{\pi(\varepsilon + k)} e^{j\pi(\varepsilon + k)} \\ &= \frac{\sin \pi\varepsilon}{\pi(\varepsilon + k)} e^{j\pi\varepsilon} \approx \frac{\sin \pi\varepsilon}{\pi k} e^{j\pi\varepsilon}. \end{aligned} \quad (32)$$

Note that when  $k = 0$ ,  $S[0] \approx (\sin \pi\varepsilon/\pi\varepsilon)e^{j\pi\varepsilon}$ . From (4), we can immediately get  $S[N - k] = S[-k]$ . Consequently,  $S[k] = -S[-k]$ , and  $S[k](-\varepsilon) = S^*[-k](\varepsilon) = S^*[N - k](\varepsilon)$ , i.e., the ICI coefficient matrix has conjugate odd symmetry.

*Proof of unitary property of  $\mathbf{S}$ :* We prove that  $\mathbf{S}$  is unitary in two steps. First, we prove that the diagonal entries of  $\mathbf{Z} = \mathbf{S}^H \mathbf{S}$ ,  $Z(m, m)$ , approach unity. Second, we prove that off-diagonal terms vanish, i.e.,  $|Z(m, m)|^2/|Z(m, n)|^2 \rightarrow \infty$  as  $\varepsilon \rightarrow 0$ .

Since  $S[N - k] = S[-k]$ , the  $\{m, n\}$ th entry of  $\mathbf{Z}$  is hence given by

$$Z(m, n) = \sum_{k=-m}^{N-1-m} S[k]S^*[k+m-n] = \sum_{k=0}^{N-1} S[k]S^*[k+m-n]. \quad (33)$$

Let us first consider diagonal entries of  $\mathbf{Z}$ . When  $m = n$ ,  $Z(m, m)$  are the diagonal entries

$$\begin{aligned} Z(m, m) &= \sum_{k=0}^{N-1} S[k]S^*[k] \\ &= S[0]S^*[0] + \sum_{k=1}^{N-1} S[k]S^*[k] \\ &= \frac{\sin^2 \pi\varepsilon}{(\pi\varepsilon)^2} + \frac{\sin^2 \pi\varepsilon}{\pi^2} \sum_{k=1}^{N-1} \frac{1}{k^2} \end{aligned} \quad (34)$$

where the second term in (34) is the Riemann's Zeta function, i.e.,  $\sum_{k=1}^{\infty} (1/k^2) = \pi^2/6$  [30]. When  $N$  is sufficiently large, the terms of  $1/k^2$ ,  $\forall k \geq N$  can be omitted. We thus have  $\sum_{k=1}^{N-1} (1/k^2) \approx \pi^2/6$ . Equation (34) can be approximated as

$$Z(m, m) \approx \sin^2(\pi\varepsilon) \left[ \frac{1}{(\pi\varepsilon)^2} + \frac{1}{6} \right] \quad (35)$$

and  $\lim_{\varepsilon \rightarrow 0} Z(m, m) = 1$ .

We next consider the off-diagonal terms. When  $m \neq n$ , since  $\mathbf{Z}$  is a Hermitian matrix, i.e.,  $Z(m, n) = Z^*(n, m)$ , it is sufficient to consider the case of  $m > n$ :

$$\begin{aligned} Z(m, n) &= S[0]S^*[m-n] + \sum_{k=1}^{N-1} S[k]S^*[k+m-n] \\ &= \frac{\sin^2 \pi\varepsilon}{\pi^2} \left[ \frac{1}{\varepsilon(m-n)} \right] + \frac{\sin^2 \pi\varepsilon}{\pi^2} \sum_{k=1}^{N-1} \frac{1}{k(k+m-n)} \\ &= \frac{\sin^2 \pi\varepsilon}{\pi^2(m-n)} \left( \frac{1}{\varepsilon} + \sum_{k=1}^{N-1} \frac{1}{k} - \sum_{k=1}^{N-1} \frac{1}{k+m-n} \right). \end{aligned} \quad (36)$$

Obviously, only when  $m - n = 1$ ,  $Z(m, n)$  can reach the maximum value  $Z(m, n)_{\max} = (\sin^2 \pi\varepsilon / \pi^2) ((1/\varepsilon) + 1 - (1/N))$ . The least power ratio of the diagonal entries to the nondiagonal entries can be given by

$$K = \frac{Z^2(m, m)}{Z^2(m, n)} > \left( \frac{1 + \frac{\pi^2 \varepsilon^2}{6}}{\varepsilon^2 + \varepsilon} \right)^2. \quad (37)$$

As  $\varepsilon \rightarrow 0$ ,  $K \rightarrow (1/\varepsilon^2)$ . The value of the normalized frequency offset has the dominant effect on the power ratio  $K$ . For instance, when  $\varepsilon = 0.3$ ,  $K > 11.1$ , which means over 90% energy is concentrated on the main diagonal. The value of  $K$  rapidly increases when  $\varepsilon$  decreases. Therefore, the ICI coefficient matrix  $\mathbf{S}$  is approximately unitary.

## REFERENCES

- [1] B. Mielczarek and W. A. Krzymieñ, "Throughput of realistic multi-user MIMO-OFDM systems," in *Proc. IEEE ISSSTA*, Sydney, Australia, Aug. 2004, pp. 434–438.
- [2] A. Bria, F. Gessler, O. Queseth, R. Stridh, M. Unbehauen, J. Wu, and J. Zander, "4th-generation wireless infrastructures: Scenarios and research challenges," *IEEE Pers. Commun.*, vol. 8, no. 6, pp. 25–31, Dec. 2001.
- [3] R. T. Derryberry, S. D. Gray, D. M. Ionescu, G. Mandyam, and B. Raghathan, "Transmit diversity in 3G CDMA systems," *IEEE Commun. Mag.*, vol. 40, no. 4, pp. 68–75, Apr. 2002.
- [4] A. S. Dakdouki, V. L. Banket, N. K. Mykhaylov, and A. A. Skopa, "Downlink processing algorithms for multi-antenna wireless communications," *IEEE Commun. Mag.*, vol. 43, no. 1, pp. 122–127, Jan. 2005.
- [5] T. Pollet, M. V. Bladel, and M. Moeneclaey, "BER sensitivity of OFDM systems to carrier frequency offset and Wiener phase noise," *IEEE Trans. Commun.*, vol. 43, no. 2/3/4, pp. 191–193, Feb./Mar./Apr. 1995.
- [6] D. J. Love, R. W. Heath, W. Santipach, and M. L. Honig, "What is the value of limited feedback for MIMO channels?" *IEEE Commun. Mag.*, vol. 42, no. 10, pp. 54–59, Oct. 2004.
- [7] M. Tomlinson, "New automatic equalizer employing modulo arithmetic," *Electron. Lett.*, vol. 7, no. 5, pp. 138–139, Mar. 1971.
- [8] H. Harashima and H. Miyakawa, "Matched-transmission technique for channels with intersymbol interference," *IEEE Trans. Commun.*, vol. COM-20, no. 4, pp. 774–780, Aug. 1972.
- [9] R. F. H. Fischer, C. Windpassinger, A. Lampe, and J. B. Huber, "Tomlinson–Harashima precoding in space–time transmission for low-rate backward channel," in *Proc. IEEE IZS*, Zurich, Switzerland, Feb. 2002, vol. 7, pp. 1–6.
- [10] —, "Space–time transmission using Tomlinson–Harashima precoding," in *Proc. ITGSCC*, Berlin, Germany, Jan. 2002, pp. 139–147.
- [11] R. F. H. Fischer, *Precoding and Signal Shaping for Digital Transmission*. New York: Wiley, 2002.
- [12] S. H. Müller-Weinfurter, "Optimal Nyquist windowing in OFDM receivers," *IEEE Trans. Commun.*, vol. 49, no. 3, pp. 417–420, Mar. 2001.
- [13] K. Sathananthan and C. Tellambura, "Partial transmit sequence and selected mapping schemes to reduce ICI in OFDM systems," *IEEE Commun. Lett.*, vol. 6, no. 48, pp. 313–315, Aug. 2004.
- [14] A. Gorokhov and J.-P. Linnartz, "Robust OFDM receiver for dispersive time-varying channels: Equalization and channel acquisition," *IEEE Trans. Commun.*, vol. 52, no. 4, pp. 572–583, Apr. 2004.
- [15] P. Schniter, "Low-complexity equalization of OFDM in doubly selective channels," *IEEE Trans. Signal Process.*, vol. 52, no. 4, pp. 1002–1011, Apr. 2004.
- [16] Y. Zhao and S.-G. Häggman, "Intercarrier interference self-cancellation scheme for OFDM mobile communication systems," *IEEE Trans. Commun.*, vol. 49, no. 7, pp. 1185–1191, Jul. 2001.
- [17] Y. Fu and C. C. Ko, "A new ICI self-cancellation scheme for OFDM systems based on a generalized signal mapper," in *Proc. IEEE WPMC*, Honolulu, HI, Oct. 2002, pp. 995–999.
- [18] A. Stamoulis, S. N. Diggavi, and A. Al-Dahir, "Intercarrier interference in MIMO OFDM," *IEEE Trans. Signal Process.*, vol. 50, no. 10, pp. 2451–2464, Oct. 2002.
- [19] R. A. Horn and C. R. Johnson, *Matrix Analysis*. New York: Cambridge Univ. Press, 2002.
- [20] S. M. Alamouti, "A simple transmit diversity technique for wireless communications," *IEEE J. Sel. Areas Commun.*, vol. 16, no. 8, pp. 1451–1458, Oct. 1998.
- [21] V. Tarokh, H. Jafarkhani, and A. R. Calderbank, "Space-time block codes from orthogonal design," *IEEE Trans. Inf. Theory*, vol. 45, no. 5, pp. 1456–1467, Jul. 1999.
- [22] Y. Li, J. H. Winters, and N. R. Sollenberger, "Signal detection for MIMO-OFDM wireless communications," in *Proc. IEEE ICC*, Helsinki, Finland, Jun. 2001, vol. 6, pp. 3077–3081.
- [23] J. Lee, D. Toumpakaris, H.-L. Lou, and J. M. Cioffi, "Effect of carrier frequency offset on OFDM systems for multipath fading channels," in *Proc. IEEE Globecom*, Dallas, TX, Nov. 2004, vol. 6, pp. 3721–3725.
- [24] D. Shiu, G. J. Foschini, M. J. Gans, and J. M. Kahn, "Fading correlation and its effect on the capacity of multi-element antenna systems," *IEEE Trans. Commun.*, vol. 48, no. 3, pp. 502–512, Mar. 2000.
- [25] E. Yoon, J. Hansen, and A. J. Paulraj, "Space-frequency precoding for an OFDM based system exploiting spatial and path correlation," in *Proc. IEEE Globecom*, Dallas, TX, Nov. 2004, vol. 1, pp. 436–440.
- [26] Recommendation ITU-R M. 1225, International Telecommunication Union, *Guidelines for Evaluation of Radio Transmission Technologies for IMT-2000*, Feb. 1997.
- [27] LAN/MAN Standards Committee, *Wireless LAN Medium Access Control (MAC) and Physical Layer (PHY) Specifications: High-Speed Physical Layer in the 5 GHz Band*, Sep. 1999, Piscataway, NJ: IEEE Std. 802.11a.
- [28] G. L. Stüber, J. R. Barry, S. W. McLaughlin, Y. G. Li, M. A. Ingram, and T. G. Pratt, "Broadband MIMO-OFDM wireless communications," *Proc. IEEE*, vol. 92, no. 2, pp. 271–294, Feb. 2004.
- [29] Y.-S. Choi, P. J. Voltz, and F. A. Cassara, "On channel estimation and detection for multicarrier signals in fast and selective Rayleigh fading channels," *IEEE Trans. Commun.*, vol. 49, no. 8, pp. 1375–1387, Aug. 2001.
- [30] I. S. Gradshteyn and I. M. Ryzhik, *Table of Integrals, Series, and Products*, 6th ed. San Diego, CA: Academic Press, 2000.

**Yu Fu** received the B.Sc. degree in electrical engineering from the Beijing University of Posts and Telecommunications, Beijing, China, in 1999 and the M.Sc. degree in electrical engineering from the National University of Singapore, Singapore, in 2002. She is currently working toward the Ph.D. degree in the Department of Electrical and Computer Engineering, University of Alberta, Edmonton, AB, Canada.

From 1999 to 2000, she was with China United Telecommunications, Ltd., Beijing, where she was involved in long-distance network measurements, SS7 signaling testing, and analysis. In 2003, she was with the MRD Technologies Pte., Ltd., Singapore, working on the design and development of PDAs and smartphones. Her research interests include transceiver optimization, equalization and preprocessing techniques, and wireless and multicarrier systems.

**Chintha Tellambura** (SM'02) received the B.Sc. degree (with first-class honors) from the University of Moratuwa, Moratuwa, Sri Lanka, in 1986, the M.Sc. degree in electronics from the University of London, London, U.K., in 1988, and the Ph.D. degree in electrical engineering from the University of Victoria, Victoria, BC, Canada, in 1993.

He was a Postdoctoral Research Fellow with the University of Victoria (1993–1994) and the University of Bradford (1995–1996). He was with Monash University, Melbourne, Australia, from 1997 to 2002. Currently, he is Professor with the Department of Electrical and Computer Engineering, University of Alberta, Edmonton, AB, Canada. His research interests include coding, communication theory, modulation, equalization, and wireless communications.

Prof. Tellambura is an Associate Editor for both the IEEE TRANSACTIONS ON COMMUNICATIONS and the IEEE TRANSACTIONS ON WIRELESS COMMUNICATIONS. He was Chair of the Communication Theory Symposium in Globecom'05 held in St. Louis, MO.

**Witold A. Krzymień** (A'79–M'79–SM'93) received the M.Sc. Eng. and Ph.D. degrees, both in electrical engineering, from the Poznań University of Technology, Poznań, Poland, in 1970 and 1978, respectively. He received a Polish national award of excellence for his Ph.D. dissertation.

Since April 1986, he has been with the Department of Electrical and Computer Engineering, University of Alberta, Edmonton, AB, Canada, where he currently holds the endowed Rohit Sharma Professorship in communications and signal processing. In 1986, he was one of the key research program architects of the newly launched TR Labs, Canada's largest industry–university–government precompetitive research consortium in the Information and Communication Technology area, headquartered in Edmonton. His research activity has been closely tied to the consortium ever since.

Over the years he has also done collaborative research work with Nortel Networks, Ericsson Wireless Communications, German Aerospace Centre (DLR- Oberpfaffenhofen), Telus Mobility, and the University of Padova (Italy). He held visiting research appointments at Twente University of Technology (Enschede, The Netherlands; 1980–1982), Bell-Northern Research (Montréal, PQ, Canada; 1993–1994), Ericsson Wireless Communications (San Diego, CA; 2000), Nortel Networks Harlow Laboratories (Harlow, U.K.; 2001), and the Department of Information Engineering at the University of Padova (2005). His research is currently focused on wideband high throughput packet data access for mobile and nomadic users, employing multicarrier signaling, multiple antenna techniques and link adaptation, as well as on the related MAC and network layer issues of hybrid ARQ, packet scheduling, and relaying.

Dr. Krzymień is a Fellow of the Engineering Institute of Canada and a licensed Professional Engineer in the Provinces of Alberta and Ontario, Canada. From 1999 to 2005, he was the Chairman of Commission C (Radio Communication Systems and Signal Processing) of the Canadian National Committee of Union Radio Scientifique Internationale (URSI), and from 2000 to 2003, he was the Associate Editor for Spread Spectrum and Multi-Carrier Systems of the IEEE TRANSACTIONS ON COMMUNICATIONS. Since 2002, he has been a member of the Editorial Board of *Wireless Personal Communications* (Springer). He received the 1991/1992 A. H. Reeves Premium Award from the Institution of Electrical Engineers (U.K.) for a paper published in the *IEE Proceedings, Part 1*.